Multiscale modeling and numerical analyses of the electric conductivity of CNT/polymer nanocomposites taking into account the tunneling effect

Xiaoxin Lu, Lionel Pichon, Jinbo Bai

Received: 27 April 2020 | Revised: 8 May 2021 | Accepted: 13 August 2021

DOI: 10.1002/jnm.2955

SPECIAL ISSUE PAPER

WILEY

Multiscale modeling and numerical analyses of the electric conductivity of CNT/polymer nanocomposites taking into account the tunneling effect

Xiaoxin Lu[1] | **Lionel Pichon**[2,3] | **Jinbo Bai**[4]

[1]Shenzhen Institute of Advanced Electronic Materials, Shenzhen Institutes of Advanced Technology, Chinese Academy of Sciences, Shenzhen, P.R. China

[2]CentraleSupélec, CNRS, Laboratoire de Génie Électrique et Électronique de Paris, Université Paris-Saclay, Gif-sur-Yvette, France

[3]CNRS, Laboratoire de Génie Électrique et Électronique de Paris, Sorbonne Université, Paris, France

[4]CentraleSupélec, CNRS, Laboratoire Mécanique des Sols, Structures et Matériaux, Université Paris-Saclay, Gif-sur-Yvette, France

Correspondence
Xiaoxin Lu, Shenzhen Institute of Advanced Electronic Materials, Shenzhen Institutes of Advanced Technology, Chinese Academy of Sciences, Shenzhen 518103, P.R. China.
Email: luxx@siat.ac.cn

Funding information
SIAT Innovation Program for Excellent Young Researchers, Grant/Award Number: E1G045; French National Research Agency, Grant/Award Number: ANR-11-IDEX-0003; LabEx LaSIPS, Grant/Award Number: ANR-10-LABX-0032-LaSIPS

Abstract

Tunneling effect plays a significant part in the extremely low electric percolation threshold and large conductivity of carbon nanotube (CNT)/polymer nanocomposites, which allows electric conduction between two CNTs separated at nanometric distances. In this work, a numerical model taking into account the nonlinear tunneling effect is proposed to evaluate the effective electric conductivity of CNT nanocomposites. The nonlinear finite element formulation is introduced, as well as the definitions of effective quantities for homogenization. Moreover, the CNTs are modeled by highly conducting line segments in order to avoid meshing the thin cylindrical tubes. With this technique, the percolation behavior of the composites has been simulated, and the effects of barrier height, CNT length distribution, CNT aspect ratio as well as alignment have been estimated. It turns out that the barrier height dominates the maximum electric conductivity, while the CNT aspect ratio determines the percolation threshold value, respectively. In addition, the anisotropic behavior is obtained by aligning the CNTs, which also results in higher percolation threshold compared with randomly distributed CNTs. Finally, the results are validated by available experimental data.

KEYWORDS

carbon nanotubes (CNTs), electric conductivity, finite element method (FEM), nanocomposites, percolation threshold, tunneling effect

1 | INTRODUCTION

In the past decade, carbon nanotubes (CNTs) have been of great interest as filler in polymers due to their excellent electrical and thermal properties, superior mechanical properties, high aspect ratio, and lightweight.[1–3] CNT-based nanocomposites have demonstrated numerous extraordinary properties, such as high electrical conductivity, low

percolation threshold, and good dielectric and mechanical properties.[4–9] The percolation threshold is the lowest concentration of filler at which insulating material is converted to conductive material. It has been reported that the effective electrical conductivity of CNT-enhanced polymer composites obeys percolation-like power law attributed to the formation of conductive CNT networks,[10] which is dominated by the tunneling effect after percolation threshold.[11,12] The tunneling effect is a quantum phenomenon that allows the electric conduction across small isolating barriers between two highly conducting fillers. When the characteristic distance between CNTs is at nanometric scale, the corresponding tunneling current plays an important role in the formation of the current path together with the conductive CNTs, leading to an increase of several orders of magnitude of the electric conductivity at extremely low volume fractions of CNTs denoting the percolation threshold.[13–15] In recent studies, the percolation threshold of CNT/polymer nanocomposites has been reported as low as 0.019 vol%.[16]

Many experimental efforts have been made, indicating that the electrical conductivity and percolation threshold of the CNT/polymer nanocomposites are significantly influenced by various parameters, such as the CNT type and aspect ratio,[17–19] synthesis method and treatment,[20–22] as well as polymer type[23,24] and dispersion method.[25,26] Moreover, the effect of CNT alignment on the electric conductivity of the nacocomposites has also been researched,[27,28] showing anisotropic behavior and demonstrating that the highly aligned CNTs rarely touch each other and thus do not form conductive pathways at small loading. However, the experimental measurements cannot be able to deeply explain the physical characteristics in the microstructures of nanocomposites.

For better understanding of the electrical phenomenon and the design purpose of smart structural applications, both analytical and numerical studies have also been conducted in this area. Ounaies et al.[29] present a simple analytical model based on the continuum theory in which the nanotubes are modeled as capped cylinders of high aspect ratio. Zare et al.[30] proposed a power-law model for characterizing the electrical conductivity of CNT nanocomposites. The other analytical approaches based on micromechanics are also provided in predicting the electrical properties and percolation threshold of CNT nanocomposties, including Hashin-Shtrikman upper bound, Ponte Castañeda-Willis theory, Mori-Tanaka method and Halpin-Tsai model,[31–36] where the CNTs are modeled as ellipsoidal inclusions uniformly distributed in 3D space. Kale et al.[37–39] modeled the CNTs as rod-like fillers, which is dispersed by RSA algorithm following Monte Carlo relaxation, and simulated the effect of filler alignment as well as the mixture of various nanofillers on the nanocomposites using the tunneling-percolation model. However, the analytical approaches show obvious limitations in the quantitative predictions of electrical properties and in the explanation of local characteristics of the microstructures. Thus, the numerical methodologies are required to better understand the local phenomenon and the effect of material parameters or morphology on the effective electric conductivity. Most of the numerical models are developed based on the statistical resistor network theory and Monte Carlo simulation.[40–46] The CNT curling has been described by separating the CNT into several elementary segments and using higher order functions such as spline functions or a helical shape in some works.[41,47–49] The effect of CNT aggregation has also been discussed by Hu et al.[41] It should be noted that tunneling effect plays an important role in the numerical simulation of the electrical conductivity of nanocomposites. For instance, Monte Carlo simulations have been employed by Li et al.[43] for simulating the electrical conductivities of percolating CNT networks, in which the tunneling resistance is calculated by Simmons' formula, assuming a rectangular potential barrier in the insulating film between CNTs. Another method to describe the tunneling resistance based on the electron transport theory has also been widely used,[44–46] where Landauer-Büttiker formula[50,51] is employed taking into account its transmission probability parameter and channel number. Although these models can provide the accurate predictions compared with experimental results and some discussion on the effect of CNT morphology, few involves the nonlinear tunneling effect and gives a deep view of local electric conduction.

In present work, we present a new technique of numerical methodology based on finite element method to study the effective conductivity of CNT/polymer nanocomposites as well as their percolation threshold. The representative volume element (RVE) containing randomly distributed or aligned CNTs are generated, and the FEM simulations taking into account the nonlinear tunneling effect are developed where the distances between CNTs are well described by the introduction of distance function. In addition, the CNTs are modeled by highly conducting line segments in the model according to their high aspect ratio, in order to avoid meshing the thin cylindrical shape. It should be noted that the morphology of polymer matrix in the composite is not taken into account, thus the phase separation[52–54] in the polymer blends which may result from the introduction of CNTs is not observed and considered in the present work.

The paper is organized as follows. In Section 2, the generation of the RVEs of CNTs/polymer nanocomposite is described, and the multiscale model is presented as well as the homogenization procedure based on FEM. In Section 3, we apply the present model to analyze the effective conductivities and percolation threshold of CNT/polymer nanocomposites after the determination of appropriate RVE size. The effect of barrier height between CNT and polymer

matrix, CNT length distribution, CNT aspect ratio as well as the alignment of CNTs are studied in detail. Finally, a general conclusion is given in Section 4.

2 | MULTISCALE MODELING OF THE ELECTRICAL BEHAVIOR OF CNT/POLYMER COMPOSITES

A representative volume element (RVE) is defined in a domain Ω whose external boundary is denoted by $\partial\Omega$, as shown in Figure 1A. The RVE with side length of L contains N straight CNTs randomly distributed in the polymer matrix, associated to Γ_n $(n=1,2,...,N)$. The conduction mechanism according to tunneling effect is introduced between the neighboring CNTs when their shortest distance is at nanoscale. The generation of the microstructures and the numerical modeling are described in the following part.

2.1 | Generation of CNT/polymer nanocomposites

In this work, each CNT is assumed to be straight with the length of l, and the diameter of D. The aspect ratio $\eta = l/D$ denotes the ratio between the length of CNT and its diameter. The aspect ratio can be altered by changing either the length l or the diameter D. The random sequential addition (RSA) algorithm is employed to generate the random microstructures of CNT/polymer nanocomposites. This algorithm works well to obtain equilibrium configurations at small filler volume fraction as in the present work. However, it should be noted that at larger fillings the procedure could be problematic, and the Metropolis algorithm should be used to equilibrate the system.[55]

As depicted in Figure 1B, the head point of ith CNT is firstly generated randomly as

$$\left(x_i^0, y_i^0, z_i^0\right) = L \times (\text{rand}, \text{rand}, \text{rand}), \tag{1}$$

where i is the index of ith CNT and 'rand' denotes uniformly generated random number in the interval $[0,1]$. The orientation of each CNT is monitored by azimuthal angle φ_i and polar angle θ_i, which are randomly generated by.[56]

$$\varphi_i = 2\pi \times \text{rand} \tag{2}$$

$$\theta_i = \cos^{-1}((1-\cos\theta_{max}) \times \text{rand} + \cos\theta_{max}). \tag{3}$$

It should be noted that θ_{max} is the maximum alignment angle which controls the extent of alignment.[44] Specifically, if $\theta_{max} = \pi/2$, the distribution of CNTs is random and isotropic; if $\theta_{max} = 0$, the CNTs are perfectly aligned.

Thus, with the contribution of head point, azimuthal, and polar angles, the end point of ith CNT can be obtained as

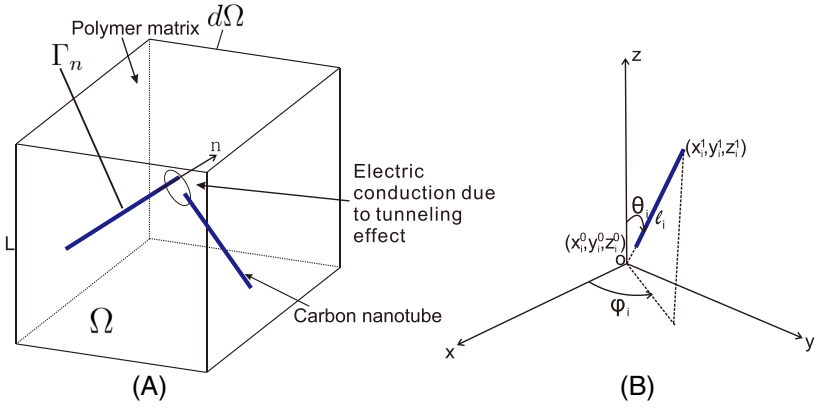

FIGURE 1 (A) RVE model of the CNT-polymer nanocomposite. (B) ith CNT in space

$$\left(x_i^1, y_i^1, z_i^1\right) = \left(x_i^0 + l_i \sin\theta_i \cos\varphi_i, y_i^0 + l_i \sin\theta_i \sin\varphi_i, z_i^0 + l_i \cos\theta_i\right). \tag{4}$$

where l_i is the length of ith CNT. The length of CNT follows a Weibull distribution,[44,57] and the probability density function is given as

$$f(x) = abx^{b-1}e^{-ax^b}, \quad \text{for } x > 0, \tag{5}$$

where a is the scale parameter and b is the shape parameter. The cumulative distribution function is

$$F(x) = 1 - e^{-\left(\frac{x}{a}\right)^b}, \quad \text{for } x > 0. \tag{6}$$

Therefore, l_i can be generated by

$$l_i = F^{-1}(\text{rand}). \tag{7}$$

All the CNTs can be described by their head points and end points. However, it should be noted that when the ending point of a CNT located outside the RVE, it will penetrate the boundary planes. By applying periodical boundary condition, the CNT will be separated to several segments and the external parts will be relocated to the RVE.

Another important point in this work is that the generation of CNTs should avoid overlap and contact of each pair of CNTs. Specifically, the following approach is employed. Firstly, we generated the head points of all the CNTs randomly in the RVE. Then the orientation of each CNT is determined one by one. As for ith CNT, once the position and orientation are determined, the shortest distance, $\mathbf{p}$, between this CNT and the other CNTs are calculated. If the minimum value of $\mathbf{p}$, p_{ij}, is less than D, the ith and jth CNTs are considered to be in contact. In this case, the orientation angles of ith CNT are rejected and have to be generated again until all the values of $\mathbf{p}$ is larger than D.

2.2 | Continuum model of the electrical behavior in CNT/polymer nanocomposites

In this model, the total electric power within the domain Ω, $\overline{W}$, which consists of the contribution of both polymer matrix and CNTs, is defined by

$$2\overline{W} = \int_{\Omega} \omega^m(\mathbf{x}) d\Omega + \int_{\Gamma} \omega^c(\mathbf{x}) d\Gamma, \tag{8}$$

where Γ denotes collectively the lines associated with CNTs and the density functions of polymer matrix (ω^m) and CNTs (ω^c), are expressed by

$$\omega^m(\mathbf{x}) = \mathbf{j}(\mathbf{x}) \cdot \mathbf{E}(\mathbf{x}), \quad \omega^c(\mathbf{x}) = \mathbf{j}^c(\mathbf{x}) \cdot \mathbf{E}^c(\mathbf{x}). \tag{9}$$

In the first equation in Equation (9), $\mathbf{E}(\mathbf{x}) = -\nabla\phi(\mathbf{x})$ is the electric field, $\mathbf{j}(\mathbf{x})$ is the current density vector and $\phi(\mathbf{x})$ is the electric potential. Taking into account tunneling effect, it satisfies:

$$\mathbf{j} = \begin{cases} \sigma^m \mathbf{E} & \text{if } d(\mathbf{x}) \geq d_{cutoff}, \\ \mathcal{G}(\mathbf{E}, d)\dfrac{\mathbf{E}}{|\mathbf{E}|} & \text{if } d(\mathbf{x}) < d_{cutoff}, \end{cases} \tag{10}$$

where $\boldsymbol{\sigma}^m$ is the electric conductivity tensor of the polymer matrix when neglecting tunneling effect, d_{cutoff} is a cut-off distance above which the tunneling effect can be neglected and $\mathcal{G}$ is defined by Simmons.[58]

$$\mathcal{G}(\mathbf{E},d)=\frac{2.2e^3|\mathbf{E}|^2}{8\pi h\Phi_0}\exp\left(-\frac{8\pi}{2.96he|\mathbf{E}|}(2m)^{\frac{1}{2}}\Phi_0^{\frac{3}{2}}\right)+\left[3\cdot\frac{(2m\Phi_0)^{\frac{1}{2}}}{2}\right](e/h)^2|\mathbf{E}|\exp\left[-\left(\frac{4\pi d}{h}\right)(2m\Phi_0)^{\frac{1}{2}}\right]. \tag{11}$$

Φ_0 is the energy barrier height that electrons cross, d is the distance between a pair of CNTs, and h, e, and m denote Plank's constant, the charge of an electron and a material parameter, respectively. The tunneling effect conduction is nonlinear which has been described in detail in.[59] According to Equation (10), the direction of the tunneling current is assumed to be the same as the direction of local electric field in the corresponding tunneling region. It should be noted that for a metal–insulator–metal junction, the J-V curve can be divided into three regimes: direct tunneling, field emission, and space-charge-limited regime. Zhang et al.[60,61] have indicated that Simmons' equation is only accurate in the direct tunneling regime, since the electron space charge potential and the electron exchange-correction potential inside the thin insulator films are ignored. They have further developed a self-consistent model taking into account the effects of both space charge and exchange-correction potential, which provide accurate estimations of the tunneling current in other regimes. In this work, we focus on the modeling approach from the mathematical point of view, and the direct tunneling stage is taken into account due to small applied electric field and the large barrier height ($\Phi_0 \geq 5$ eV). Hence, the Simmons' formula is employed directly for simplicity.

In the second equation in Equation (9), the superscript c denotes line quantities for CNTs, e.g., $\mathbf{j}^c$ is the line current density and $\mathbf{E}^c=-\nabla_\Gamma\phi$ is the line electric field on CNTs which is calculated by taking the gradient of electric potential on the two nodes of the line element. CNTs can be considered as rolled-up sheets of graphene sheets, with a finite diameter denoted by D. However, due to the very high aspect ratio of CNTs, which can be of the order of 10^3 between its length and diameter, it is cumbersome to model them as cylindrical volume domains regarding meshing problems in the extremely thin cylinders. To overcome this problem, we propose to replace the CNTs with finite diameter by highly conducting lines. The local constitutive relationships relating $\mathbf{j}^c$ with $\mathbf{E}^c$ is defined in the CNTs by

$$\mathbf{j}^c(\mathbf{x})=\boldsymbol{\sigma}^c\mathbf{E}^c, \tag{12}$$

where $\boldsymbol{\sigma}^c$ denotes the equivalent line electric conductivity of CNT and is dependent on the diameter D through:

$$\boldsymbol{\sigma}^c=\frac{\pi D^2}{4}\mathbf{S},\quad \mathbf{S}=\sigma_0^c\mathbf{n}\otimes\mathbf{n}. \tag{13}$$

In Equation (13), $\mathbf{n}$ is the unit direction vector of CNT and σ_0^c denotes electric conductivity of the CNT along the $\mathbf{n}$ direction (see Refs. [62–64] for more details).

Minimizing Equation (8) with respect to the displacement field, and using Equations (9) and (10), we obtain the weak form which can be solved by the finite element method:

$$\int_\Omega \mathbf{j}(\phi)\cdot\nabla(\delta\phi)d\Omega-\int_\Gamma \nabla_\Gamma\phi\cdot\boldsymbol{\sigma}^c\nabla_\Gamma(\delta\phi)d\Gamma=0, \tag{14}$$

where $\delta\phi\in H^1(\Omega)$, $\delta\phi=0$ over $\partial\Omega$, and $\phi\in H^1(\Omega)$, ϕ satisfying the periodic boundary conditions over $\partial\Omega$

$$\phi(\mathbf{x})=-\overline{\mathbf{E}}\cdot\mathbf{x}+\widetilde{\phi}(\mathbf{x})\qquad\text{on }\partial\Omega \tag{15}$$

and where $\widetilde{\phi}(\mathbf{x})$ is a periodic function over Ω, such as $\langle\widetilde{\phi}(\mathbf{x})\rangle=0$.

The effective electric conductivity tensor $\overline{\boldsymbol{\sigma}}$ is defined as:

$$\overline{\boldsymbol{\sigma}}(\overline{\mathbf{E}})=\frac{\partial\overline{\mathbf{J}}(\overline{\mathbf{E}})}{\partial\overline{\mathbf{E}}}, \tag{16}$$

where $\overline{\mathbf{J}}$ is the effective current density expressed by:

$$\overline{\mathbf{J}} = \frac{1}{V}\left(\int_{\Omega} \mathbf{j}(\mathbf{x}) d\Omega + \int_{\Gamma} \mathbf{j}^{c}(\mathbf{x}) d\Gamma\right), \tag{17}$$

and $\overline{\mathbf{E}}$ is the effective electric field given by:

$$\overline{\mathbf{E}} = \frac{1}{V}\int_{\Omega} \mathbf{E}(\mathbf{x}) d\Omega, \tag{18}$$

where V is the volume of Ω.

In this model, the tunneling effect plays an important part in the electric conduction, and it is dependent on a distance d between CNTs. In what follows, we present a choice of definition for the distance function $d(\mathbf{x})$ in Equation (11), which can be computed at all nodes of the mesh once before the calculations for a given distribution of CNTs within the RVE. Firstly, in a given CNT composite system, the CNTs are taken as randomly distributed line segments in a RVE. We calculate the shortest distance between each pair of CNTs and link the corresponding two points by an additional line segment (see the dash line in Figure 2). GMSH mesh generator[65] is used to create the two-point mesh of the line segments conforming with matrix tetrahedra. Consider an arbitrary point $\mathbf{x} \in \Omega$ and a set of points lying on all the CNTs denoted by $\mathbf{x}^{\Gamma}$, we define the preliminary distance $d^{0}(\mathbf{x})$ as

$$d^{0}(\mathbf{x}) = \min_{\substack{\mathbf{x}^{\Gamma} \in \Gamma^{i} \\ i=1,2,\ldots,N}} \left\|\mathbf{x} - \mathbf{x}^{\Gamma}\right\| + \min_{\substack{\mathbf{x}^{\Gamma} \in \Gamma^{j} \\ j=1,2,\ldots,N,\ j \neq i}} \left\|\mathbf{x} - \mathbf{x}^{\Gamma}\right\|. \tag{19}$$

That is to say, for a given node $\mathbf{x}$ in the mesh, we first compute the distance with all N CNTs, then $d^{0}(\mathbf{x})$ is defined as the sum of the two smallest distances between this point and two neighboring CNTs. For instance, as shown in Figure 2, the distances d_0^1, d_0^2, and d_0^3 represent the shortest distance between CNTs Γ^1, Γ^2, Γ^3, and the point $\mathbf{x}$, respectively. Thus, the preliminary distance $d^{0}(\mathbf{x})$ for this point is the sum of d_0^1 and d_0^2, which are the smallest values in the set of d_0^i, $i = 1, 2, 3$. Finally, considering the diameter of the CNTs, the distance function $d(\mathbf{x})$ is given by

$$d(\mathbf{x}) = \max\left\{d_{vdW}, d^{0}(\mathbf{x}) - D\right\}, \tag{20}$$

where d_{vdW} denotes the van der Waals separation distance. It should be noted that the separation between a pair of CNTs should always be larger than d_{vdW} according to the Pauli exclusion principle.[66,67] The unit of the RVE size and the cutoff distance of tunneling effect are μm and nm, respectively. Due to this enormous gap of orders of magnitude, the nodes of which $d(\mathbf{x})$ is below the cutoff distance of tunneling effect are mainly located on the CNTs.

3 | NUMERICAL ANALYSIS AND DISCUSSION

It has been reported that the conductivity of the multiwalled carbon nanotubes ranges from 20 to 2×10^{7} S/m.[68] In all the following calculations, the electric conductivities of the polymer and CNTs are taken as $\sigma^{m} = 1 \times 10^{-10}$ S/m and

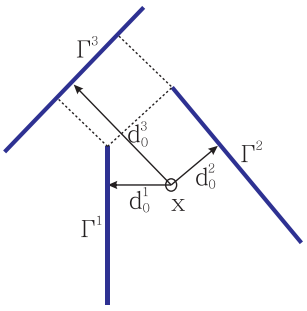

FIGURE 2 Distances of a point $\mathbf{x}$ from surrounding CNTs to compute the distance $d^{0}(\mathbf{x})$

$\sigma_0^c = 1 \times 10^6$ S/m.[69] The length of a CNT is $l = 2\,\mu$m, and the aspect ratio $\eta = l/D$ changes with various diameter values D. Periodical boundary condition is employed and the applied electric field is $\overline{E}_i = 0.125$ V/μm, $i = x,y,z$. The cutoff distance of tunneling effect $d_{\text{cutoff}} = 1.7$ nm, and the van der Waals separation distance is chosen to be $d_{vdW} = 3.4$ Å.[67]

3.1 | RVE size analysis

In this example, we analyze the statistical convergence of the effective conductivity of the composites and its convergence as a function of RVE size. The averaged effective electric conductivity tensor component $\overline{\sigma}_k$ of N realizations is defined by

$$<\overline{\sigma}_k>_N = \frac{1}{N}\sum_{i=1}^{N}\overline{\sigma}_k^i, \tag{21}$$

where $\overline{\sigma}_k^i$ is the value of effective electric conductivity tensor component $\overline{\sigma}_k$ of the ith realization. Figure 4 shows the averaged effective electric conductivity tensor component $\overline{\sigma}_x$ versus the number of realizations under various RVE sizes ranging from 2.5 to 7 μm. The diameter of CNTs $D = 50$ nm, and the aspect ratio $\eta = 40$. For each size of cube domain defining the RVE, the realizations have the same CNT volume fraction ($f = 2.2$ vol%). The barrier height between CNTs and polymer matrix is set to be 10 eV. It demonstrates that the averaged effective electric conductivity finally converged to a certain value when the number of the realizations is large enough. It is obvious that the larger the RVE size is, the less realizations are required to reach the convergence. For instance, when the side length of RVE is 2.5 μm, the averaged value of effective conductivity converges at nearly 600 realizations, while the side length of RVE increases to 7 μm, 10 realizations are enough to reach the convergence value.

Furthermore, to determine the RVE size, we plot the averaged effective electric conductivity and its ranges as a function of the side length of RVE in Figure 3. For each point, the number of random realizations is large enough to reach the statistic convergence according to the results in Figure 4. It shows that the dispersion of the results decreases when the size of the domain increases. The mean values converge when the side length of the RVE is roughly 5 μm, which is the value we use in the following analysis.

3.2 | Effective electrical conductivity and percolation threshold

In this section, the proposed methodology is used to investigate the influence of CNT volume fraction on the effective electric conductivity of the composites. The side length of the cubic RVE is 5 μm, and the volume fraction of CNTs is

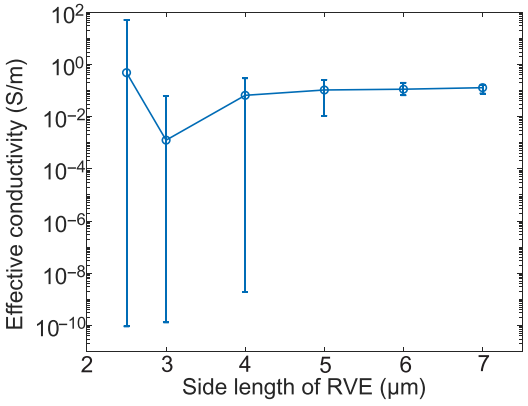

FIGURE 3 Mean values and the ranges of effective conductivity versus the side length of RVE. For each case, the number of realizations insures the convergence of the mean value. The aspect ratio of CNTs is $\eta = l/D = 40$, the CNTs volume fraction is 2.2 vol%, the barrier height $\Phi_0 = 10$ eV, and the applied electric field is 0.125 V/μm

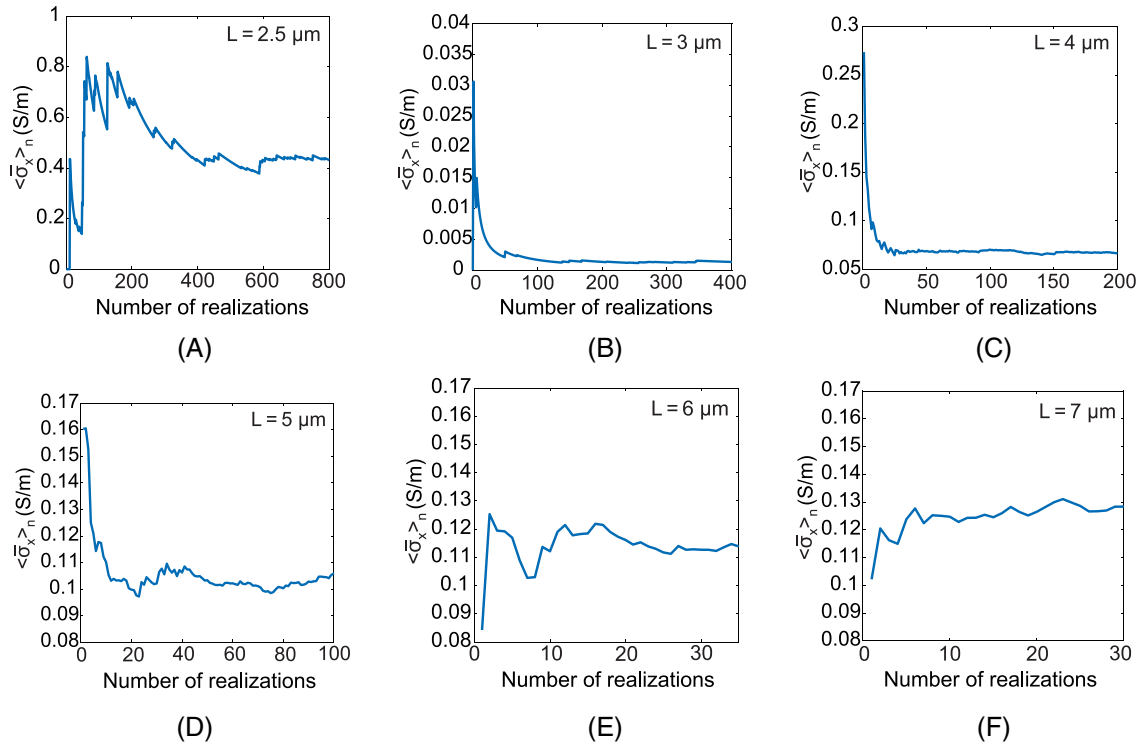

FIGURE 4 Averaged effective conductivity $\overline{\sigma}_x$ as a function of the number of realizations at the condition of various RVE size. (A) $L = 2.5$ μm; (B) $L = 3$ μm; (C) $L = 4$ μm; (D) $L = 5$ μm; (E) $L = 6$ μm; (F) $L = 7$ μm. The aspect ratio CNTs $\eta = l/D = 40$, the CNTs volume fraction is 2.2 vol%, the barrier height $\Phi_0 = 10$ eV, and the applied electric field is 0.125 V/μm

increased by increasing the number of introduced CNTs in the domain. Several realizations with various CNT volume fraction ranging from 0.1 to 0.8 vol% are shown in Figure 5, where the CNTs are randomly distributed whose aspect ratio is 100. The barrier height between the matrix and CNTs is taken as $\Phi_0 = 10$ eV. The numerical results are provided in Figure 6. Taking into account the tunneling effect, the numerical values of $\overline{\sigma}_x$, $\overline{\sigma}_y$ and $\overline{\sigma}_z$ are plotted as a function of CNTs volume fraction in Figure 6A–C, where the average values are obtained for 40 realizations, and their ranges are also presented. It indicates that the electric conductivity of CNT nanocomposite increases with the CNT volume fraction. It should be noted that a sharp rise of the conductivity of several orders of magnitude occurs at about 0.4 vol%, where the mean values turn to be over 10^{-8} S/m. The percolation threshold is the minimum content of conductive filler in the insulating matrix which is characterized by a sharp increase in conductivity due to the formation of conductive network and realize an insulator-to-conductor transition in the composites. Thus, we estimate the percolation threshold in the CNTs nanocomposite is around 0.4 vol%. It is obvious to see that the deviations of the conductivities of the realizations are much higher when the CNTs volume fraction is around the percolation threshold.

Furthermore, for better comparison, we have superimposed the mean values of $\overline{\sigma}_x$, $\overline{\sigma}_y$, and $\overline{\sigma}_z$ in Figure 6D and compared with the average value $\frac{1}{3}\left(\overline{\sigma}_x + \overline{\sigma}_y + \overline{\sigma}_z\right)$ when the tunneling effect is neglected. Firstly, it shows that the mean electric conductivities along the three axes (x, y, and z) are almost the same in the random structures, which leads to an isotropic behavior in the electric properties. Noting that in our model, the polymer matrix is insulating and the CNTs are not in contact with each other, it can be concluded that the tunneling effect is responsible of the sharp increase of electrical conductivity and the extremely low percolation threshold in CNTs nanocomposites.

In order to better demonstrate the importance of tunneling effect on the percolation behavior, the current density field in the polymer matrix of a random microstructure is plotted in Figure 7 for both with and without tunneling effect, respectively. The side length of RVE cube is 2.5 μm, the volume fraction of CNTs is $f = 1.58$ vol%, with aspect ratio $l/D = 40$. The applied electric field is $\overline{E}_x = 0.125$ V/μm. It can be seen in Figure 7A that neglecting the tunneling effect, the maximum current density in the polymer matrix is less than 10^{-9} A/mm^2, indicating that the composite is insulating. By introducing the tunneling effect, the tunneling current in the local matrix between neighboring CNTs can be observed in Figure 7B, which is even 10^9 times larger than in Figure 7A. In this case, the current paths can be formed

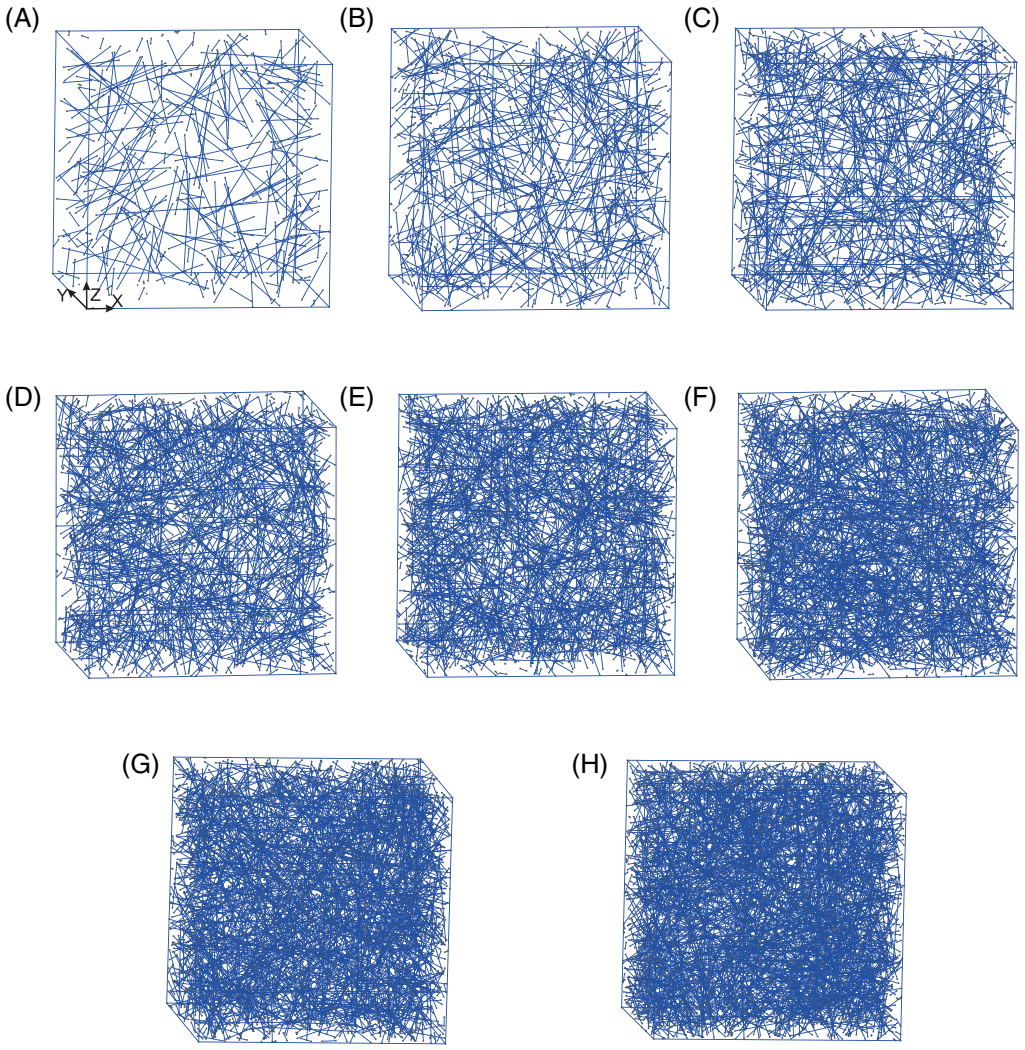

FIGURE 5 Realizations of microstructures for different CNT volume fractions, where the CNTs are randomly distributed in RVE. $l/D = 100$. (A) f = 0.1 vol%. (B) f = 0.2 vol%. (C) f = 0.3 vol%. (D) f = 0.4 vol%. (E) f = 0.5 vol%. (F) f = 0.6 vol%. (G) f = 0.7 vol%. (H) f = 0.8 vol%

according to the link of local tunneling current which finally results in the insulator-to-conductor transition. In addition, the enhancement of the electric flux can be observed near CNTs in both the cases.

3.3 | Effect of CNT length distribution

Figure 8 shows the effective conductivity versus CNT volume fraction under various length distribution. Each point in the curve is computed by taking the average of 40 realizations with randomly dispersed CNTs. Two shapes of Weibull distributions are provided for the length of CNTs, which are also presented in Figure 8. According to Equation (5), the parameters are set to: $a = 2.256$ μm, $b = 2.4$, and $a = 2.178$ μm, $b = 5$, respectively. The average length of CNT in both cases is 2 μm. The effective conductivities of the nanocomposites with CNT of constant length ($l = 2$ μm) are also computed as comparison. In addition, the diameter of CNT is 50 nm, the barrier height is set to be $\Phi_0 = 10$ eV. The results show that the distribution of CNT length does not affect the percolation threshold of the nanocomposites, which is about 1.1 vol%. In addition, it should be noted that the increase of the dispersion of CNT length leads to a growth of the effective conductivity after percolation threshold, but its effect is very tiny. Hence, the length of the CNTs is considered a constant in the following computations.

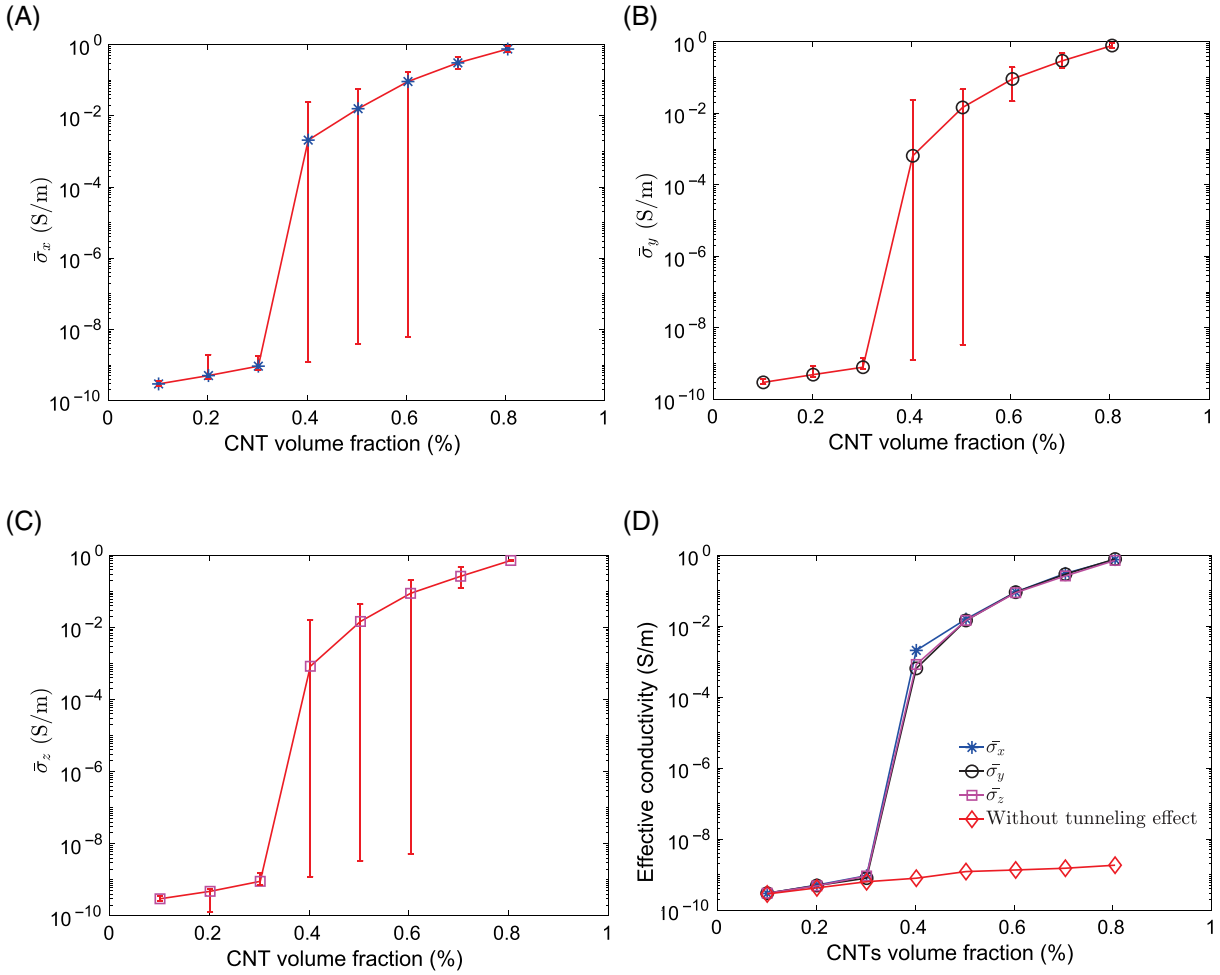

FIGURE 6 Effective conductivities tensor components (mean value and range) as a function of the CNT volume fraction, $\overline{E} = 0.125$ V/μm, $\Phi_0 = 10$ eV, $l/D = 100$. (A) $\overline{\sigma}_x$, (B) $\overline{\sigma}_y$, (C) $\overline{\sigma}_z$, (D) Comparison with the case in which tunneling effect is neglected

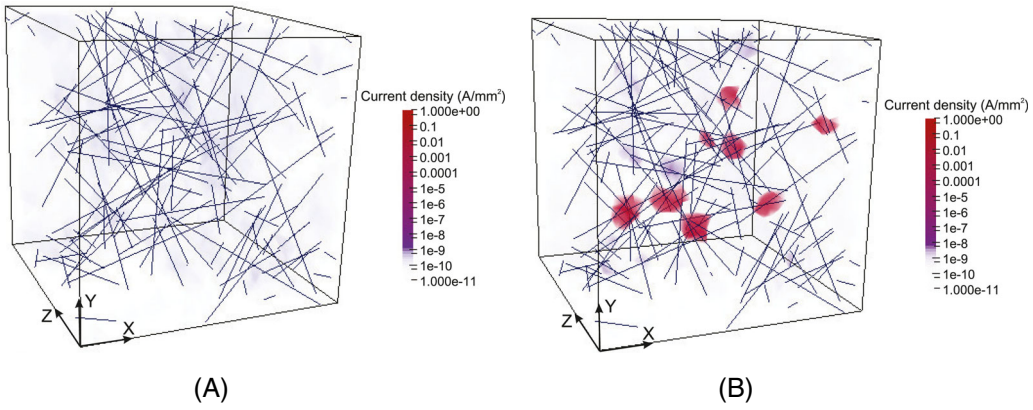

FIGURE 7 Current density in the polymer matrix of microstructure with CNT volume fraction $f = 1.58$ vol%, $l/D = 40$. Side length of RVE L = 2.5 μm, $\overline{E}_x = 0.125$ V/μm: (A) without tunneling effect; (B) considering tunneling effect. The values below the minimum of scale bar are set to transparency. The ParaView post-treatment software was used[70]

3.4 | Effect of CNT aspect ratio

Next, we study the effect of CNTs aspect ratio on the electric properties by estimating the percolation threshold of the nanocomposites with CNTs of various aspect ratios using the proposed model. In Figure 9, the electric conductivity

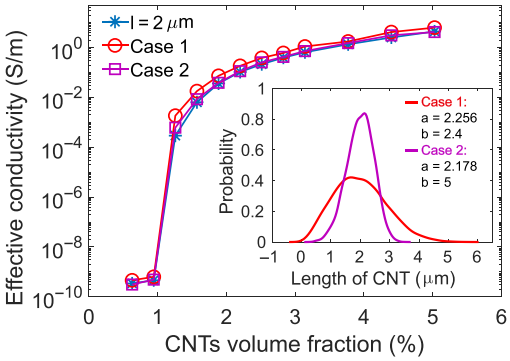

FIGURE 8 Effective conductivity as a function of the CNT volume fraction under various CNT length distributions: two cases in which CNT length follows Weibull distribution in different shapes with the average length $<l> = 2$ μm, and the other one in which CNT length is a constant as $l = 2$ μm. D = 50 nm, $\overline{E}_x = 0.125$ V/μm, $\Phi_0 = 10$ eV

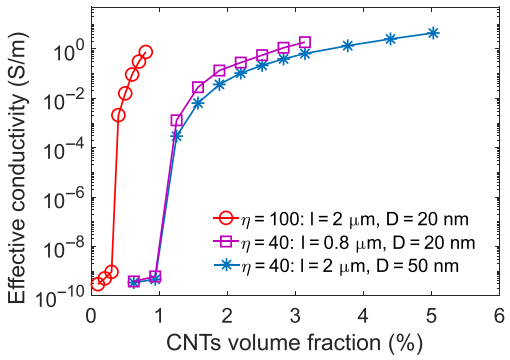

FIGURE 9 Effective conductivity as a function of the CNT volume fraction under various CNT aspect ratio l/D, $\overline{E}_x = 0.125$ V/μm, $\Phi_0 = 10$ eV

$\overline{\sigma}_x$ is computed as a function of CNTs volume fraction for different aspect ratios $l/D = 40$ and 100, respectively. The barrier height is $\Phi_0 = 10$ eV. Each point in the figure is computed by taking the average of 40 realizations with randomly distributed CNTs. Two various methods are employed to change the aspect ratio of CNT from 100 to 40: either fix length l and increase diameter D, or fix diameter D and decrease length l. The effect of these two cases in the modeling on the electric properties of CNT nanocomposites are compared. According to the results, we can notice that the two presented methods changing the aspect ratio of CNT result in a same value of percolation threshold. The percolation threshold is clearly dependent on the aspect ratio of CNTs, and the larger aspect ratio results in lower percolation threshold. The obtained percolation thresholds for $l/D = 40$ and 100 are 1.1 and 0.4 vol%, respectively. Moreover, comparing the two provided cases which have the same CNT aspect ratio ($\eta = 40$), it can be seen that the composites with smaller scale of CNT ($l = 0.8$ μm) present higher effective electric conductivity at the same CNT content after percolation threshold. It may be attributed to the increase of the local tunneling regions according to the decrease of the length of CNT.

3.5 | Effect of Barrier height between CNT and matrix

In the following, the effects of barrier height between CNTs and polymer matrix on the electric behavior of CNTs nanocomposite are discussed. Figure 10 shows the effective conductivity component $\overline{\sigma}_x$ as a function of the CNTs volume fraction for $\Phi_0 = 5$, 10, and 15 eV, respectively. For each case, the values are averaged over 40 realizations of random distributions of CNTs within the RVE. The aspect ratio of CNTs is 100, and the applied electric field is $\overline{E}_x = 0.125$ V/μm. It should be noted that the various barrier heights do not influence the percolation threshold, but has a considerable effect on the electric conductivities of the composites whose CNTs volume fraction is above the percolation threshold. Specifically, in the three cases, the percolation threshold of the composites stays at 0.4 vol%. However,

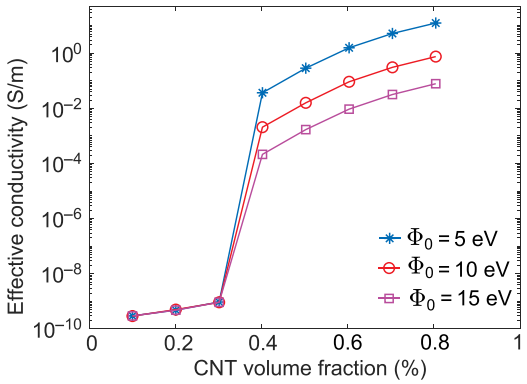

FIGURE 10 Effective conductivity versus CNT volume fraction for several barrier heights Φ_0, $\overline{E}_x = 0.125$ V/μm, $l/D = 100$

the increase in conductivity after the percolation threshold is sharper at lower Φ_0, leading to a higher maximum electric conductivity. Overall, it is obviously seen from the analysis that the barrier height plays a dominant role in the maximum electric conductivity of the composites, while the percolation threshold is mainly determined by the aspect ratio of CNT filler. Therefore, comparing with experiment results, it provides good potential in the identification of the barrier height between CNTs and polymer matrix as well as in the estimation of the CNTs aspect ratio.

3.6 | Effect of alignment of CNTs

In this section, the effect of CNT alignment on the electric conductivities of the nanocomposites is evaluated. For this purpose, we generate a series of microstructures with perfectly aligned CNTs ($\theta_{max} = 0$) whose volume fraction is ranging from 0.1 to 1.1 vol% as shown in Figure 11. The parameters of CNTs are the same as those outlined in Figure 5, i.e., the aspect ratio $l/D = 100$, the barrier height $\Phi_0 = 10$ eV, the applied electric field $\overline{E}_i = 0.125$ V/μm ($i = x,y,z$). The numerical results of effective conductivities along three main axes $\overline{\sigma}_x$, $\overline{\sigma}_y$, and $\overline{\sigma}_z$ are plotted as a function of CNTs volume fraction, respectively, in Figure 12. Each point corresponds to the mean value over 40 realizations. Moreover, we compared these data with the effective conductivity of composites composed by random distributed CNTs. According to the isotropic behavior with random distribution of CNTs, the effective conductivity of the realizations for random microstructures is denoted by $\frac{1}{3}\left(\overline{\sigma}_x + \overline{\sigma}_y + \overline{\sigma}_z\right)$.

The main features that can be taken from this figure can be summarized as follows. Firstly, the anisotropic feature of the composites with aligned CNTs is clearly captured, such as the effective conductivities in the direction normal to CNTs, $\overline{\sigma}_y$ and $\overline{\sigma}_z$, are much smaller than that in the aligned direction $\overline{\sigma}_x$. Within the CNTs volume fraction of 1 vol%, the composite is insulating in y and z directions, while transits from insulator to conductor at 0.8 vol% in the x direction, which is indicated as percolation threshold. It should be noted that with applied electric field E_x, the tunneling current is supposed to be in the same direction as E_x according to Equation (10), which is not realistic and would increase the electric current along the x direction to some extent, but would not affect the value of percolation threshold. However, according to the computational limitation, we focus on the simulation of composites with small CNT content by the finite element method, in which the material is insulating along y and z directions, i.e., the current path has not been formed in y and z directions. In this case, most of the tunneling current is formed from tip to tip of CNTs in the x direction and the error that comes from the assumption of tunneling current is reduced. If the volume fraction of aligned CNTs is high, the electric contacts by the electric tunneling in parallel CNTs can not be neglected and should be modified as presented by Banerjee et al.[71] Another conclusion is that aligning the CNTs leads to a larger percolation threshold and a sharper increase in conductivity after the percolation threshold, as compared to randomly oriented CNTs. Thus, the randomly distributed CNTs present to be more conductive than aligned CNTs at low CNT volume fraction. We are aware that as the CNT volume fraction increases, the electric conductivity of aligned CNTs may exhibit a significant increase when the current paths are also formed along y and z directions, resulting in the conductivity higher than that of the randomly distributed CNTs.

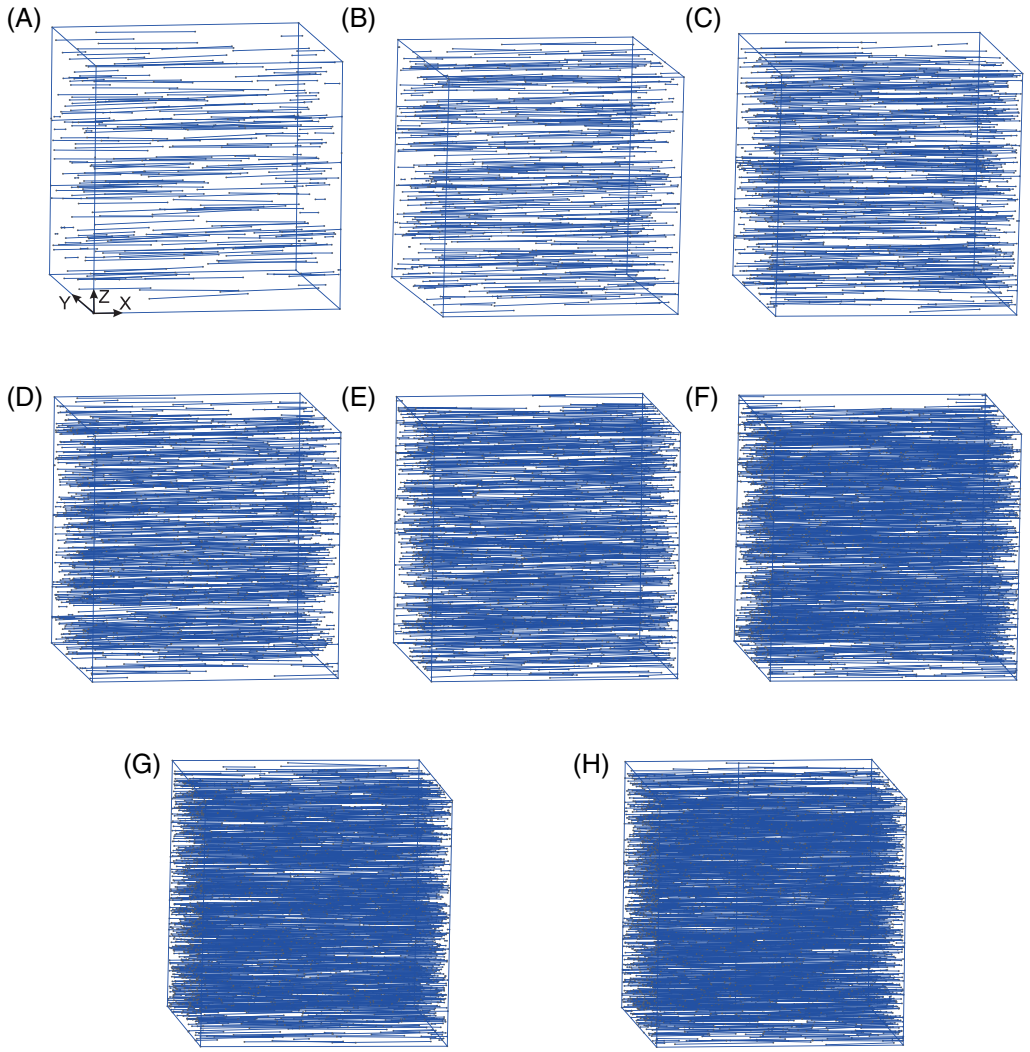

FIGURE 11 Realizations of microstructures for different CNT volume fractions, where the CNTs are aligned along X axis in RVE. $l/D = 100$. (A) f = 0.1 vol%. (B) f = 0.2 vol%. (C) f = 0.3 vol%. (D) f = 0.4 vol%. (E) f = 0.5 vol%. (F) f = 0.6 vol%. (G) f = 0.8 vol%. (H) f = 1.1 vol%

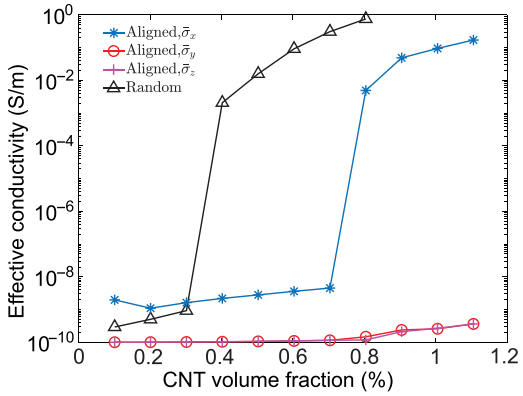

FIGURE 12 Effective conductivity tensor components as a function of CNT volume fraction for the microstructures either with randomly distributed CNTs or aligned CNTs. $\overline{E} = 0.125$ V/μm, $\Phi_0 = 10$ eV, $l/D = 100$

3.7 | Comparison between numerical and experimental results

In the following, we verify the application of the proposed model by comparing the obtained numerical results with the available experimental data reported by Ono et al.[72] and Tsuchiya et al.,[73] respectively. Figure 13 shows the electric

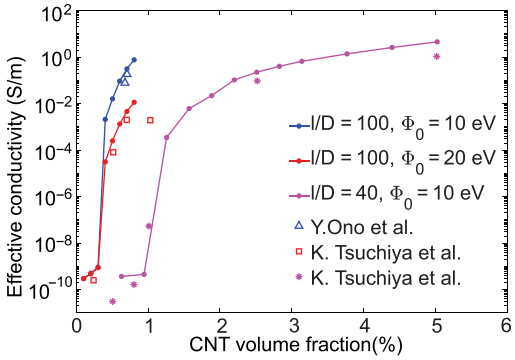

FIGURE 13 Comparison of electrical conductivity with existing experimental results[72,73]

conductivity measured as a function of CNTs volume fraction from which we can also estimate the percolation threshold. The CNTs used in the experiments are either single-walled or multiwalled carbon nanotubes in different types, whose aspect ratio ranges from 50 to 1000. Various types of CNTs and polymer matrix, as well as the different methods in the fabrication of the nanocomposites lead to different barrier height which affects the tunneling effect.

In our numerical simulation, the electric conductivity of CNTs is supposed to be 10^6 S/m, and their distribution is random in the matrix without aggregation and contact. Assuming the aspect ratio of CNTs is 100, and the barrier height is 10 eV, we can see the estimated electric conductivity after percolation threshold agrees well with the experiment results in.[72] Due to the limitation of computation time and computation cost, we focus on the electric properties around percolation threshold which we have interest in and did not go further to the composites with high CNTs volume fraction. Then keeping the aspect ratio at 100 and changing the barrier height to 20 eV, we get the numerical results in good agreement with the experiment data of the SWNTs (Super Growth)/styrene-butadiene rubber composites,[73] whose percolation threshold is measured to be about 0.5 vol%. The electric conductivities of MWNTs (Nikkiso)/styrene-butadiene rubber composite in[73] are also provided in Figure 13, whose tendency can be reproduced by our model with the barrier height of 10 eV and the CNT aspect ratio of 40. It should be noted that due to the computational limitations, the contrast of conductivities between CNTs and polymer matrix cannot be higher than 10^{16}. Therefore, the electrical conductivity of polymer matrix has to be taken as 10^{-10} S/m, which results in the discrepancy between experimental and numerical results for low CNT volume fraction before percolation threshold.

4 | CONCLUSION

In this paper, a multiscaled numerical model for predicting the electrical properties of CNTs/polymer nanocomposite has been proposed. Comparing with the analytical methods and the existing numerical models, several novelties and advantages have been presented in this work. Firstly, the nonlinear tunneling effect has been introduced for the conduction mechanism between neighboring CNTs, which is described by defining a distance function in the composite system, and associated with the local electric field as well as barrier height between various CNTs and polymer matrix. Then, the nonlinear equations have been solved by the FEM technique, where the CNTs are modeled by highly conducting line segments in order to avoid meshing the extremely thin cylinders due to their high aspect ratio. The effective electric conductivity has been finally estimated by appropriate definitions of effective quantities through homogenization. The numerical model can be used for any complicated microstructure, no matter with random distributed or aligned CNTs.

From the numerical analysis, we are able to reproduce the low percolation threshold of CNT nanocomposites which is proved mainly dependent on the tunneling effect. The simulation predictions demonstrate that the length distribution of the CNT length has a minor effect on the electric behavior of CNT nanocomposites. The increase of barrier height between CNT and polymer leads to lower maximum electric conductivity beyond percolation threshold, but has no effect in the value of percolation threshold. It indicates that the percolation threshold is determined by the aspect ratio of CNTs filler. The higher aspect ratio of CNT results in lower percolation threshold for the nanocomposites. Moreover, we report that aligning the CNTs leads to a typical anisotropic electric behavior and a larger percolation threshold compared to randomly distributed CNTs, which presents isotropy in electric conductivities. Finally, the

proposed numerical results were compared with the experimental data, showing a good agreement in both the tendency and percolation threshold value.

ACKNOWLEDGEMENTS

This work has benefited from the financial support of the LabEx LaSIPS (ANR-10-LABX-0032-LaSIPS) managed by the French National Research Agency under the "Investissements d'avenir" program (ANR-11-IDEX-0003). Xiaoxin Lu also thanks the SIAT Innovation Program for Excellent Young Researchers (E1G045).

DATA AVAILABILITY STATEMENT

Research data are not shared.

ORCID

Xiaoxin Lu https://orcid.org/0000-0003-2149-4049

REFERENCES

1. Demczyk BG, Wang YM, Cumings J, et al. Direct mechanical measurement of the tensile strength and elastic modulus of multiwalled carbon nanotubes. *Mater Sci Eng A*. 2002;334(1–2):173-178.
2. Tans SJ, Devoret MH, Groeneveld RJ, Dekker C. Electron–electron correlations in carbon nanotubes. *Nature*. 1998;394(6695):761-764.
3. Hamada N, Sawada S-i, Oshiyama A. New one-dimensional conductors: graphitic microtubules. *Phys Rev Lett*. 1992;68(10):1579-1581.
4. Geng Y, Liu MY, Li J, Shi XM, Kim JK. Effects of surfactant treatment on mechanical and electrical properties of CNT/epoxy nanocomposites. *Compos A: Appl Sci Manuf*. 2008;39(12):1876-1883.
5. Otaegi I, Aranburu N, Iturrondobeitia M, Ibarretxe J, Guerrica-Echevarria G. The effect of the preparation method and the dispersion and aspect ratio of CNTs on the mechanical and electrical properties of bio-based polyamide-4,10/CNT nanocomposites. *Polymers*. 2019;11(12):2059.
6. Cha J, Kim J, Ryu S, Hong SH. Comparison to mechanical properties of epoxy nanocomposites reinforced by functionalized carbon nanotubes and graphene nanoplatelets. *Composites*. 2019;162:283-288.
7. Zhang Q, Huang J-Q, Qian W-Z, Zhang Y-Y, Wei F. The road for nanomaterials industry: a review of carbon nanotube production, post-treatment, and bulk applications for composites and energy storage. *Small*. 2013;9(8):1237-1265.
8. Liu H, Gao J, Huang W, et al. Electrically conductive strain sensing polyurethane nanocomposites with synergistic carbon nanotubes and graphene bifillers. *Nanoscale*. 2016;8(26):12977-12989.
9. Zhang X, Yan X, He Q, et al. Electrically conductive polypropylene nanocomposites with negative permittivity at low carbon nanotube loading levels. *ACS Appl Mater Interfaces*. 2015;7(11):6125-6138.
10. Coleman JN, Curran S, Dalton A, et al. Percolation-dominated conductivity in a conjugated-polymer-carbon-nanotube composite. *Phys Rev B*. 1998;58(12):R7492-R7495.
11. Martin-Gallego M, Bernal M, Hernandez M, Verdejo R, López-Manchado MA. Comparison of filler percolation and mechanical properties in graphene and carbon nanotubes filled epoxy nanocomposites. *Eur Polym J*. 2013;49(6):1347-1353.
12. Zeng X, Xu X, Shenai PM, et al. Characteristics of the electrical percolation in carbon nanotubes/polymer nanocomposites. *J Phys Chem C*. 2011;115(44):21685-21690.
13. Hu G, Zhao C, Zhang S, Yang M, Wang Z. Low percolation thresholds of electrical conductivity and rheology in poly (ethylene terephthalate) through the networks of multi-walled carbon nanotubes. *Polymer*. 2006;47(1):480-488.
14. Ameli A, Nofar M, Park C, Pötschke P, Rizvi G. Polypropylene/carbon nanotube nano/microcellular structures with high dielectric permittivity, low dielectric loss, and low percolation threshold. *Carbon*. 2014;71:206-217.
15. Tjong SC, Liang G, Bao S. Electrical behavior of polypropylene/multiwalled carbon nanotube nanocomposites with low percolation threshold. *Scr Mater*. 2007;57(6):461-464.
16. Zhang K, Li G-H, Wang N, Guo JEA. Ultralow percolation threshold and enhanced electromagnetic interference shielding in poly(l-lactide)/multi-walled carbon nanotube nanocomposites with electrically conductive segregated networks. *J Mater Chem C*. 2017;5:9359-9369.
17. Bryning MB, Islam MF, Kikkawa JM, Yodh AG. Very low conductivity threshold in bulk isotropic single-walled carbon nanotube–epoxy composites. *Adv Mater*. 2005;17(9):1186-1191.
18. Gojny FH, Wichmann MH, Fiedler B, et al. Evaluation and identification of electrical and thermal conduction mechanisms in carbon nanotube/epoxy composites. *Polymer*. 2006;47(6):2036-2045.
19. Li J, Ma PC, Chow WS, C. K. To, Tang BZ, Kim J-K. Correlations between percolation threshold, dispersion state, and aspect ratio of carbon nanotubes. *Adv Funct Mater*. 2007;17(16):3207-3215.
20. Kim YJ, Shin TS, Do Choi H, Kwon JH, Chung Y-C, Yoon HG. Electrical conductivity of chemically modified multiwalled carbon nanotube/epoxy composites. *Carbon*. 2005;43(1):23-30.
21. Kymakis E, Amaratunga GA. Electrical properties of single-wall carbon nanotube-polymer composite films. *J Appl Phys*. 2006;99(8):084302.

22. Saeed K, Park S-Y. Preparation and properties of multiwalled carbon nanotube/polycaprolactone nanocomposites. *J Appl Polym Sci*. 2007;104(3):1957-1963.
23. Regev O, ElKati PN, Loos J, Koning CE. Preparation of conductive nanotube–polymer composites using latex technology. *Adv Mater*. 2004;16(3):248-251.
24. Andrews R, Jacques D, Minot M, Rantell T. Fabrication of carbon multiwall nanotube/polymer composites by shear mixing. *Macromol Mater Eng*. 2002;287(6):395-403.
25. Kovacs JZ, Velagala BS, Schulte K, Bauhofer W. Two percolation thresholds in carbon nanotube epoxy composites. *Compos Sci Technol*. 2007;67(5):922-928.
26. Hornbostel B, Pötschke P, Kotz J, Roth S. Single-walled carbon nanotubes/polycarbonate composites: basic electrical and mechanical properties. *Phys Status Solidi B*. 2006;243(13):3445-3451.
27. Du F, Fischer JE, Winey KI. Effect of nanotube alignment on percolation conductivity in carbon nanotube/polymer composites. *Phys Rev B*. 2005;72(12):121404.
28. Wang Q, Dai J, Li W, Wei Z, Jiang J. The effects of CNT alignment on electrical conductivity and mechanical properties of swnt/epoxy nanocomposites. *Compos Sci Technol*. 2008;68(7–8):1644-1648.
29. Ounaies Z, Park C, Wise K, Siochi E, Harrison J. Electrical properties of single wall carbon nanotube reinforced polyimide composites. *Compos Sci Technol*. 2003;63(11):1637-1646.
30. Zare Y, Rhee KY. A power model to predict the electrical conductivity of CNT reinforced nanocomposites by considering interphase, networks and tunneling condition. *Composites*. 2018;155B:11-18.
31. Seidel GD, Lagoudas DC. A micromechanics model for the electrical conductivity of nanotube-polymer nanocomposites. *J Compos Mater*. 2009;43(9):917-941.
32. Weng GJ. A dynamical theory for the Mori–Tanaka and Ponte Castañeda–Willis estimates. *Mech Mater*. 2010;42(9):886-893.
33. Pan Y, Weng G, Meguid S, Bao W, Zhu Z-H, Hamouda A. Percolation threshold and electrical conductivity of a two-phase composite containing randomly oriented ellipsoidal inclusions. *J Appl Phys*. 2011;110(12):123715.
34. Pal G, Kumar S. Multiscale modeling of effective electrical conductivity of short carbon fiber-carbon nanotube-polymer matrix hybrid composites. *Mater Design*. 2016;89:129-136.
35. Zare Y, Rhee KY, Park SJ. A developed equation for electrical conductivity of polymer carbon nanotubes (CNT) nanocomposites based on Halpin-Tsai model. *Results Phys*. 2019;14:102406.
36. Zhu JM, Zare Y, Rhee KY. Analysis of the roles of interphase, waviness and agglomeration of CNT in the electrical conductivity and tensile modulus of polymer/CNT nanocomposites by theoretical approaches. *Colloids Surf A Physicochem Eng Asp*. 2018;539:29-36.
37. Kale S, Karimi P, Sabet FA, Jasiuk I, Ostoja-Starzewski M. Tunneling-percolation model of multicomponent nanocomposites. *J Appl Phys*. 2018;123(8):085104.
38. Kale S, Sabet FA, Jasiuk I, Ostoja-Starzewski M. Tunneling-percolation behavior of polydisperse prolate and oblate ellipsoids. *J Appl Phys*. 2015;6(15):15113-15122.
39. Kale S, Sabet FA, Jasiuk I, Ostoja-Starzewski M. Effect of filler alignment on percolation in polymer nanocomposites using tunneling-percolation model. *J Appl Phys*. 2016;120:045105.
40. Grujicic M, Cao G, Roy W. A computational analysis of the percolation threshold and the electrical conductivity of carbon nanotubes filled polymeric materials. *J Mater Sci*. 2004;39(14):4441-4449.
41. Hu N, Masuda Z, Yan C, Yamamoto G, Fukunaga H, Hashida T. The electrical properties of polymer nanocomposites with carbon nanotube fillers. *Nanotechnology*. 2008;19(21):215701.
42. Yu Y, Song G, Sun L. Determinant role of tunneling resistance in electrical conductivity of polymer composites reinforced by well dispersed carbon nanotubes. *J Appl Phys*. 2010;108(8):084319.
43. Li C, Thostenson ET, Chou T-W. Dominant role of tunneling resistance in the electrical conductivity of carbon nanotube–based composites. *Appl Phys Lett*. 2007;91(22):223114.
44. Bao W, Meguid S, Zhu Z, Meguid M. Modeling electrical conductivities of nanocomposites with aligned carbon nanotubes. *Nanotechnology*. 2011;22(48):485704.
45. Bao W, Meguid S, Zhu Z, Weng G. Tunneling resistance and its effect on the electrical conductivity of carbon nanotube nanocomposites. *J Appl Phys*. 2012;111(9):093726.
46. Gong S, Zhu Z, Meguid S. Anisotropic electrical conductivity of polymer composites with aligned carbon nanotubes. *Polymer*. 2015;56:498-506.
47. Karimi P, Amiri-Hezaveh A, Ostoja-Starzewski M, Jin J-M. Electromagnetic characteristics of systems of prolate and oblate ellipsoids. *J Appl Phys*. 2017;122(18):185101.
48. Dalmas F, Dendievel RM, Chazeau L, Cavaillé J-Y, Gauthier C. Carbon nanotube-filled polymer composites. Numerical simulation of electrical conductivity in three-dimensional entangled fibrous networks. *Acta Mater*. 2006;54(11):2923-2931.
49. Shi DL, Feng XQ, Huang YGY, Hwang KC, Gao HJ. The effect of nanotube waviness and agglomeration on the elastic property of carbon nanotube-reinforced composites. *J Eng Mater Technol Trans ASME*. 2004;126(3):250-257.
50. Tamura R, Tsukada M. Electronic transport in carbon nanotube junctions. *Solid State Commun*. 1997;101(8):601-605.
51. Buldum A, Lu JP. Contact resistance between carbon nanotubes. *Phys Rev B*. 2001;63(16):161403.
52. Sharma M, Sharma K, Bose S. Segmental relaxations and crystallization-induced phase separation in pvdf/pmma blends in the presence of surface-functionalized multiwall carbon nanotubes. *J Phys Chem B*. 2013;117(28):8589-8602.

53. Lee M, Koo J, Ki H, et al. Phase separation and electrical conductivity of nanocomposites made of ether−/ester-based polyurethane blends and carbon nanotubes. *Macromol Res*. 2017;25(3):231-242.
54. Zare Y, Garmabi H, Rhee KY. Structural and phase separation characterization of poly(lactic acid)/poly(ethylene oxide)/carbon nanotube nanocomposites by rheological examinations. *Compos Part B Eng*. 2018;144:1-10.
55. Miller A. Mark, on structural correlations in the percolation of hard-core particles. *J Chem Phys*. 2009;131(6):1421.
56. Hu N, Karube Y, Yan C, Masuda Z, Fukunaga H. Tunneling effect in a polymer/carbon nanotube nanocomposite strain sensor. *Acta Mater*. 2008;56(13):2929-2936.
57. Wang S, Liang Z, Wang B, Zhang C. Statistical characterization of single-wall carbon nanotube length distribution. *Nanotechnology*. 2006;17(3):634-639.
58. Simmons JG. Generalized formula for the electric tunnel effect between similar electrodes separated by a thin insulating film. *J Appl Phys*. 1963;34(6):1793-1803.
59. Lu X, Yvonnet J, Detrez F, Bai J. Multiscale modeling of nonlinear electric conductivity in graphene-reinforced nanocomposites taking into account tunnelling effect. *J Comput Phys*. 2017;337:116-131.
60. Zhang P. Scaling for quantum tunneling current in nano-and subnano-scale plasmonic junctions. *Sci Rep*. 2015;5:9826.
61. Banerjee S, Zhang P. A generalized self-consistent model for quantum tunneling current in dissimilar metal-insulator-metal junction. *AIP Adv*. 2019;9(8):085302.
62. Bossavit A. Small parameter problems in eddy-current theory: a review, and case-study on how to avoid meshing small air-gaps. *IEEE Trans Magn*. 1996;32(3):729-732.
63. Gu S, He Q-C. Interfacial discontinuity relations for coupled multifield phenomena and their application to the modeling of thin interphases as imperfect interfaces. *J Mech Phys Solids*. 2011;59(7):1413-1426.
64. Yvonnet J, He Q-C, Toulemonde C. Numerical modelling of the effective conductivities of composites with arbitrarily shaped inclusions and highly conducting interface. *Compos Sci Technol*. 2008;68(13):2818-2825.
65. Geuzaine C, Remacle J-F. Gmsh: a 3-D finite element mesh generator with built-in pre-and post-processing facilities. *Int J Numer Methods Eng*. 2009;79(11):1309-1331.
66. Hertel T, Walkup RE, Avouris P. Deformation of carbon nanotubes by surface van der waals forces. *Phys Rev B*. 1998;58(20):13870-13873.
67. Girifalco L, Hodak M, Lee RS. Carbon nanotubes, buckyballs, ropes, and a universal graphitic potential. *Phys Rev B*. 2000;62(19):13104-13110.
68. Ebbesen T, Lezec H, Hiura H, Bennett J, Ghaemi H, Thio T. Electrical conductivity of individual carbon nanotubes. *Nature*. 1996;382(6586):54-56.
69. Takeda T, Shindo Y, Kuronuma Y, Narita F. Modeling and characterization of the electrical conductivity of carbon nanotube-based polymer composites. *Polymer*. 2011;52(17):3852-3856.
70. Ayachit U. *The Paraview Guide: a Parallel Visualization Application*. Kitware, Inc; 2015.
71. Banerjee S, Luginsland J, Zhang P. A two dimensional tunneling resistance transmission line model for nanoscale parallel electrical contacts. *Sci Rep*. 2019;9(1):1-14.
72. Ono Y, Aoki T, Ogasawara T. Mechanical and electrical properties of carbon-nanotube composites, in: Proceedings of the 48th Conference on Structural Strength, Japan; 2006, p. 141.
73. Tsuchiya K, Sakai A, Nagaoka T, Uchida K, Furukawa T, Yajima H. High electrical performance of carbon nanotubes/rubber composites with low percolation threshold prepared with a rotation–revolution mixing technique. *Compos Sci Technol*. 2011;71(8):1098-1104.

How to cite this article: Lu X, Pichon L, Bai J. Multiscale modeling and numerical analyses of the electric conductivity of CNT/polymer nanocomposites taking into account the tunneling effect. *Int J Numer Model*. 2021; e2955. doi:10.1002/jnm.2955